



ELSEVIER

Contents lists available at ScienceDirect

## Journal of Magnetism and Magnetic Materials

journal homepage: [www.elsevier.com/locate/jmmm](http://www.elsevier.com/locate/jmmm)

# Ab-initio investigation of spin-dependent transport properties in Fe-doped armchair graphyne nanoribbons



S. GolafroozShahri, M.R. Roknabadi\*, N. Shahtahmasebi, M. Behdani

Department of Physics, Ferdowsi University of Mashhad, Mashhad, Iran

## ARTICLE INFO

## Article history:

Received 10 February 2016

Received in revised form

10 June 2016

Accepted 23 June 2016

Available online 24 June 2016

## Keywords:

Spintronic

Magnetic impurity

Density functional theory

Graphyne nanoribbons

Non-equilibrium Green function

## ABSTRACT

An ab-initio study on the spin-polarized transport properties of H-passivated Fe-doped graphyne nanoribbons is presented. All the calculations were based on density functional theory (DFT). Doping single magnetic atom on graphyne nanoribbons leads to metallicity which can significantly improve the conductivity. The currents are not degenerate for both up and down spin electrons and they are considerably spin-polarized. Therefore a relatively good spin-filtering can be expected. For configurations with geometric symmetry spin-rectifying is also observed. Therefore they can be applied as a dual spin-filter or a dual spin-diode in spintronic equipment.

© 2016 Elsevier B.V. All rights reserved.

## 1. Introduction

By increasing development of investigations on low dimensional electronic systems, and study of their electronic and spintronic properties, quantum transport properties of low dimensional systems have been of particular interest.

Many physicists believe that spintronic will be one of the most significant branches of future technological researches. So far, the focus of spin dependent studies has been on graphene based nano structures [1–10] such as nanoribbons [11], nanotubes [12,13] and fullerenes [14]. In which, applying gate voltage [15] putting the sample between two ferromagnetic electrodes [16–23], inducing defects, doping or substituting impurities into structures to produce spin-polarized states [7,24–29] have been employed for further understanding on their spin-dependent properties.

Graphyne (Gy), another two dimensional allotrope of carbon, has been the subject of increasing studies due to its special structural, electrical, optical and mechanical properties. Gys, which were predicted by Baughman in 1987 [30], have the same symmetry as graphene with hexagonal carbon rings ( $sp^2$  hybridized C atom) and acetylenic linkage ( $sp$  hybridized C atom) [31]. The presence of  $sp$  carbon atoms allows the formation of multiple lattice types of graphyne sheets with different symmetries called  $\alpha$ ,  $\beta$ ,  $\gamma$  and 6-6-12 graphyne [32].

\* Corresponding author.

E-mail address: [roknabad@um.ac.ir](mailto:roknabad@um.ac.ir) (M.R. Roknabadi).

Recent theoretical researches indicated that Graphyne has been proven to possess phenomenal electronic properties as graphene [33–36]. The structural and electronic properties of graphyne nanoribbons (GyNRs), which would be formed by cutting Gy sheets, are strongly dependent on the edge chirality (armchair, zigzag) and their widths.

Few researches have been devoted to study the influence of magnetic impurity on electronic and transport properties of graphyne nano structures [37,38]. Regarding promising application of Graphyne family as a spintronic device requires more extensive studies.

Introduction of impurities to carbon-base nano structures can produce spin-dependent characteristics and spin-polarized states, which makes them suitable for spintronic applications [7,27,39]. Although the electronic, optical, mechanical and transport properties of graphyne nanoribbons have been studied [32,40–43], the effect of magnetic impurity on their properties have not yet been examined. In this context, the influence of a single magnetic impurity on spin-polarized transport of graphyne nanoribbons is the subject of present study. Also, the dependency of its behavior to the width of ribbons has been shown.

In this work, ab initio calculations were used to study Fe-doped narrow graphyne nanoribbons, passivated by hydrogen, to investigate the spin-dependent transport properties in the framework of density functional theory. Also the impact of AGyNRs width variation on transport behavior was addressed.

## 2. Model and method

To investigate the electronic properties of Fe-doped armchair graphyne nanoribbons (n-AGyNR), in which “n” indicate the number of hexagonal rings in the width of ribbon, we performed ab-initio calculations with spin-polarized density functional theory (DFT) using OpenMX simulation package [44]. DFT method plays a substantial role in study of nano scale structure properties. The exchange and correlation effect was approximated with generalized gradient approximation (GGA) of Perdew–Burke–Ernzerhof (PBE) [45] and the core electrons are substituted by Troullier–Martins norm-conserving pseudo potential. A Monkhorstpack scheme [46] with  $1 \times 1 \times 5$  mesh points in k-space was considered. An energy cutoff of 150 Ry was chosen to expand atomic wave functions. All atoms were relaxed till the residual forces on each atom become less than 0.02 eV/Å. To avoid the possible interaction of nanoribbons with adjacent system, an enough vacuum layer (12 Å) was chosen in the non-periodic directions (Fig. 1).

For transport calculations we perform Non-equilibrium Green's Function (NEGF) as implanted in the TranMain module in OpenMX package. The device structure illustrated in (Fig. 2) is divided into three parts, including two semi-infinite electrodes and a scattering region.

The spin-polarized current through the scattering region is calculated by Landauer–Büttiker formula [47]. To quantify the spin-polarization, we also calculated the spin filter efficiency (SFE) of current, which is defined as:

$$SFE = \frac{|I_{\uparrow} - I_{\downarrow}|}{|I_{\uparrow} + I_{\downarrow}|} \times 100 \quad (1)$$

where  $I_{\uparrow}$  and  $I_{\downarrow}$  are the currents of up and down spin, respectively.

## 3. Results and discussions

We calculate and compare the stability of  $n=1$ ,  $n=2$  and  $n=3$  AGyNR (Fig. 1) in various possible site of doped Fe atom to find out the most stable ground state. The results show that regardless of Fe atom location, ribbons with Fe impurity have magnetic ground

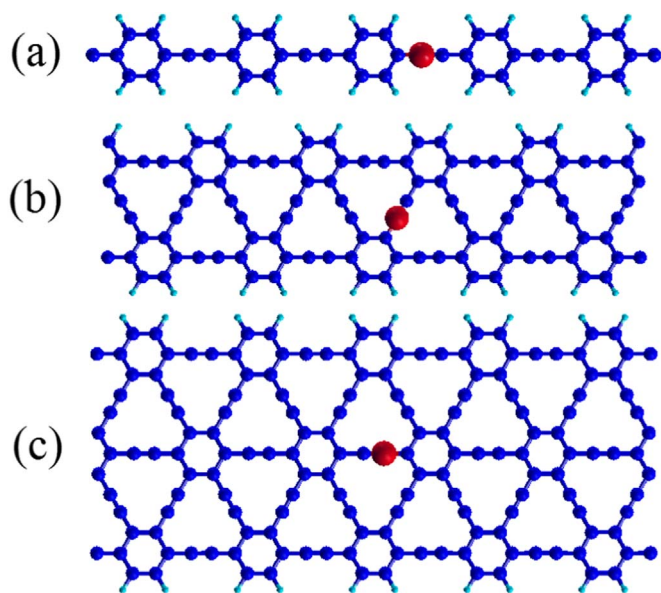


**Fig. 1.** Schematic representation of (a)  $n=1$ , (b)  $n=2$  and (c)  $n=3$  Fe-doped AGyNR. The dark blue, light blue and red spheres represent C, H and Fe atoms, respectively. (For interpretation of the references to color in this figure legend, the reader is referred to the web version of this article.)

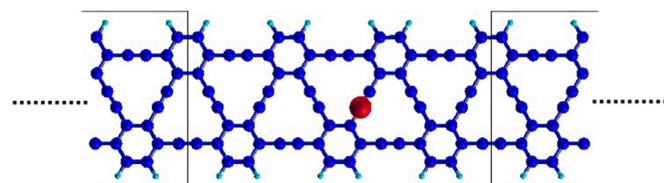


**Fig. 2.** Schematic representation of Fe-doped nanoribbon connected to two semi-infinite electrodes for transport calculation.

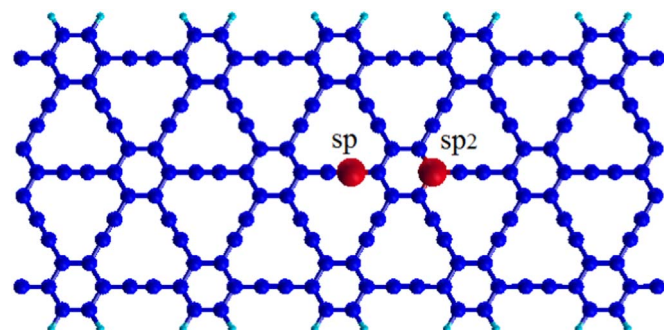


**Fig. 3.** Schematic representation of two possible doping sites in AGyNRs mentioned by sp and  $sp^2$ .

**Table 1**

The total energy of all considered pristine and Fe-doped n-AGyNRs for  $n=1$ ,  $n=2$  and  $n=3$  after relaxation.

Total energy (eV)	sp-site	$sp^2$ -site
1-AGyNR	−453.787	−449.433
2-AGyNR	−1011.672	−991.403
3-AGyNR	−1569.633	−1554.479

**Table 2**

The measured bond lengths of all considered pristine and Fe-doped n-AGyNRs for  $n=1$ ,  $n=2$  and  $n=3$  after relaxation.

Bond length (Å)	C–C (sp–sp)	C–C (sp– $sp^2$ )	Fe–C (sp–sp)	Fe–C (sp– $sp^2$ )
1-AGyNR	1.2538	1.4465	1.7800	1.9446
2-AGyNR	1.2538	1.4467	1.7710	1.9435
3-AGyNR	1.2541	1.4424	1.7212	1.8703

state. In the studied nanoribbons there are two different doping configuration which are shown in (Fig. 3) labeled by sp and  $sp^2$ . After complete relaxation of system, the total energy of each three investigated nanoribbons ( $n=1$ ,  $n=2$  and  $n=3$  Fe-doped AGyNRs) in both doping sites were calculated (see Table 1), and the results reveal the most stable configuration is achievable by substitution of sp carbon with Fe atom, as it exhibits lowest total energy.

The bonding lengths of all structure are listed in (Table 2); where Fe atom bond length with its nearest neighbor is about 1.7 Å and 1.9 Å for sp and  $sp^2$  substitutions with small variations. The C–C bond length becomes larger after Fe doping and the lattice symmetry is disturbed. Furthermore, the geometry of GyNRs would not be severely distorted.

Band structure and density of state (DOS) of Fe-doped armchair n-graphyne nanoribbons (n-AGyNR) was studied and compared with pure ones. The results are shown in (Fig. 4). All pure nanoribbons are semiconductor, with energy band gap of about 1.6, 1.3 and 1.0 eV for  $n=1$ ,  $n=2$  and  $n=3$  AGyNR, respectively. In addition, the band gaps are located near to the X point in the first Brillouin zone. It was found that, similar to graphene [48–50], the band gaps of the studied samples shows a descending trend with increasing nanoribbons width; which is in good agreement with

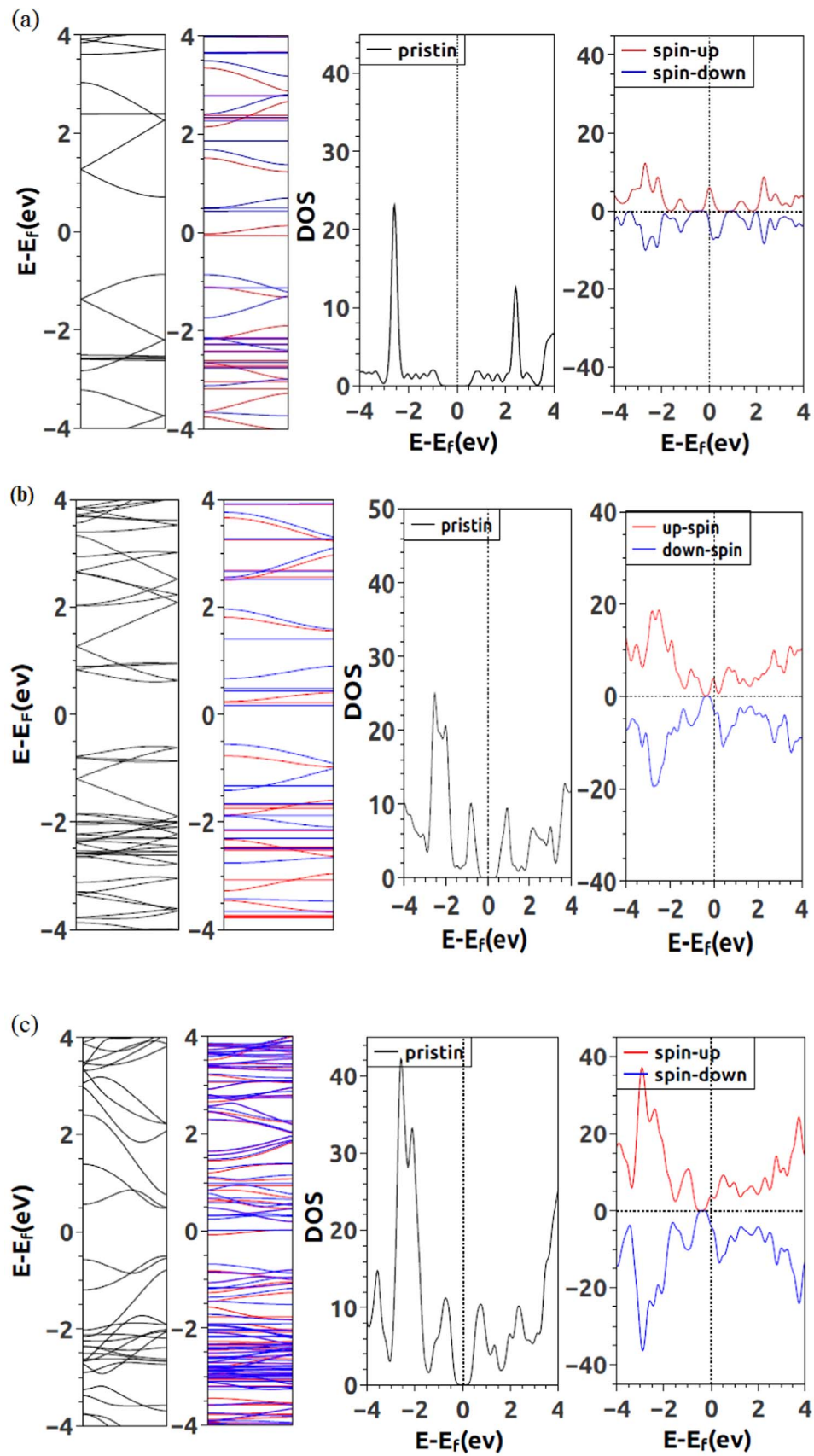


**Fig. 4.** Band structure and total density of states (DOS) for (a)  $n=1$ , (b)  $n=2$  and (c)  $n=3$  pristine and Fe-doped AGyNR. Pristine, up spin and down spin states correspond to black, red and blue lines, respectively. (For interpretation of the references to color in this figure legend, the reader is referred to the web version of this article.)

**Table 3**

The calculated Fermi level of all considered pristine and Fe-doped n-AGyNRs for  $n=1$ ,  $n=2$  and  $n=3$ .

n-AGyNR	$n=1$ (pure)	$n=2$ (pure)	$n=3$ (pure)	$n=1$ (Fe- doped)	$n=2$ (Fe- doped)	$n=3$ (Fe- doped)
Fermi level (eV)	-3.58	-4.07	-3.91	-3.53	-3.80	-3.62

other reports [51].

Evidently, metal atoms could be good electron donors because of their contribution of valance electrons to conduction band of GyNRs. According to the band structure diagrams, in Fe-doped nanoribbons, increasing the amount of electrons caused an impurity state above Fermi level near conduction band of primitive structure. The conducting channels, explaining the band structure of materials, from valance to conduction band, indicate the metallic nature of Fe-doped nanoribbons.

Furthermore, we find that up spin and down spin electronic states are not degenerate and they are spin-polarized. The existence of additional electronic states, from delocalized Fe electrons, crosses the Fermi level leads to metallicity. These additional states are imputed to delocalized Fe-3d electrons. The reason is that a small amount of charge transfer takes place from Fe to C atom and consequently the Fermi level is shifted downwards; calculated Fermi level are presented in (Table 3).

The overlap between  $3p^6 4s^2 3d^6$  orbitals of Fe atom and  $2s^2 2p^2$  orbitals of C atoms gives rise to changing DOS spectrum. In DOS spectrum of pristine and Fe-doped nanoribbons, the positions of DOS curves are in agreement with the electronic band structures of ribbons. It is clear from DOS spectrum; pure nanoribbons are semiconductor, in accordance with the previous finding [50], while Fe-doped nanoribbons DOS is nonzero in the Fermi level that shows metallic behavior like corresponding band structure. All the nanoribbons have spin-polarized electronic states unlike the pure ones (which is related their nonmagnetic ground state). These properties provide the possibility of spin polarization and spin filtering effect in a device.

Furthermore, we find by increasing the width of nanoribbons, the DOS peaks intensity increases as well, indicating better conductivity of them. As can be seen, for 1-AGyNR, a sharp peak is observed at the Fermi level for up spin DOS spectrum, formed by contribution of Fe-s, Fe-p and Fe-3d orbital. While, for 2-AGyNR and 3-AGyNR, down spin electrons have sharper peaks at the Fermi level, confirmed by corresponding band structures which show down spin state is near to Fermi level.

To study the conductivity of single magnetic metal on armchair

**Table 4**

The threshold voltage of all considered pristine and Fe-doped n-AGyNRs for  $n=1$ ,  $n=2$  and  $n=3$ .

n-AGyNR	$n=1$ (pure)	$n=2$ (pure)	$n=3$ (pure)	$n=1$ (Fe- doped)	$n=2$ (Fe- doped)	$n=3$ (Fe- doped)
Threshold voltage (V)	1.8	1.4	1.2	1.4	1.3	1.1

graphyne nanoribbons, spin-polarized transport calculations were performed for Fe-doped GyNRs sandwiched between two pure AGyNR electrodes. At each bias voltage, the up and down spin currents were calculated self-consistently under the Non-equilibrium condition using the Landauer–Büttiker formula.

The currents for up spin ( $I_+$ ) and down spin ( $I_-$ ) of Fe-doped n-AGyNR as well as pure ones are plotted versus the applied bias voltage ( $V_b$ ) in (Fig. 5). For pure and Fe-doped GyNRs, apparent current appears when the bias voltage exceeds the band gap. All pure n-AGyNRs display semiconductor behavior which is in accordance with their band structures and density of states, in which the threshold voltages are about 1.8 V, 1.4 V and 1.2 V for  $n=1$ ,  $n=2$ , and  $n=3$ , respectively (Table 4). It is obvious that, by doping magnetic impurity on studied n-AGyNRs, the conductance of nanoribbons is improved because as can be seen, in all considered nanoribbons threshold voltage decreased in Fe-doped cases (1.4 V, 1.3 V and 1.1 V for  $n=1$ ,  $n=2$ , and  $n=3$ , respectively).

According to  $I$ - $V$  curves of Fe-doped n-AGyNRs, the current for both up and down spins are not degenerate, so it is considerably spin-polarized. When the bias voltage becomes larger than the threshold voltage, clearly visible that the current has two parts for up and down spin electrons. This is because the impurity states of doping atom induce extra transport channels.

Now we turn to the behavior of the current–voltage ( $I$ - $V$ ) of our Fe-doped GyNRs. The curves in (Fig. 6) describe the spin-polarized currents as a function of the applied bias ( $I$ - $V$  curve) for Fe-doped AGyNRs at the bias range from  $-2.0$  V to  $2.0$  V. Two different features observed: spin filtering and spin-rectifying effects. For Fe-doped 1-AGyNR, the up spin current through the ribbon increases rapidly, especially when the bias become higher than threshold voltage about 1.4 V. While the down spin current is obviously smaller than that of up spin electrons and increases slowly with the increase of bias in the entire voltage range, this occurs because the resonances for the up spin state are closer to the Fermi level. As can be seen, the individual currents of up and down spins are symmetric around zero bias. The up spin electrons can easily pass through the system when the positive bias is higher than threshold voltage, while it is almost forbidden within the bias range

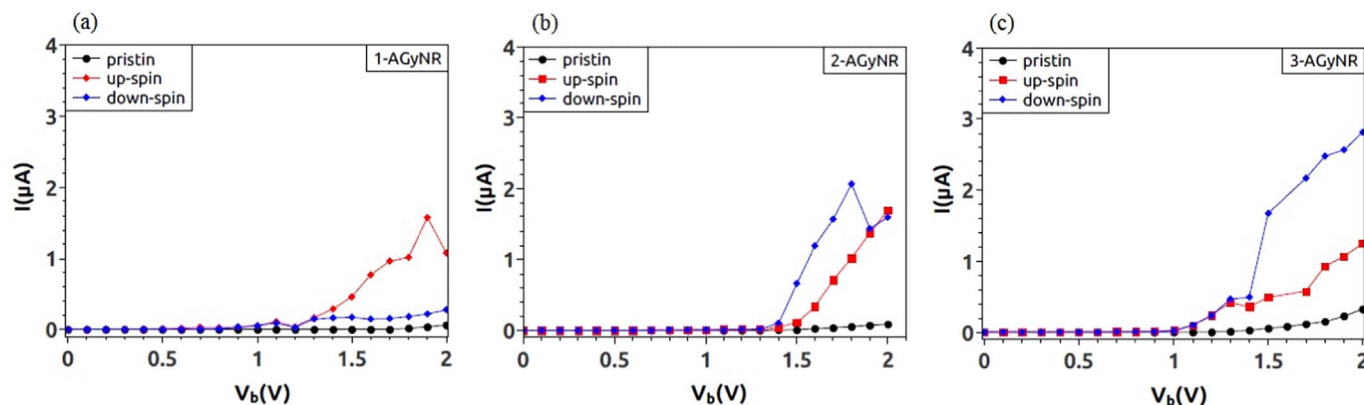


**Fig. 5.** The  $I$ - $V$  curves of (a)  $n=1$ , (b)  $n=2$  and (c)  $n=3$  pristine and Fe-doped AGyNR in positive bias voltages. Pristine, up spin and down spin states correspond to black, red and blue lines, respectively. (For interpretation of the references to color in this figure legend, the reader is referred to the web version of this article.)

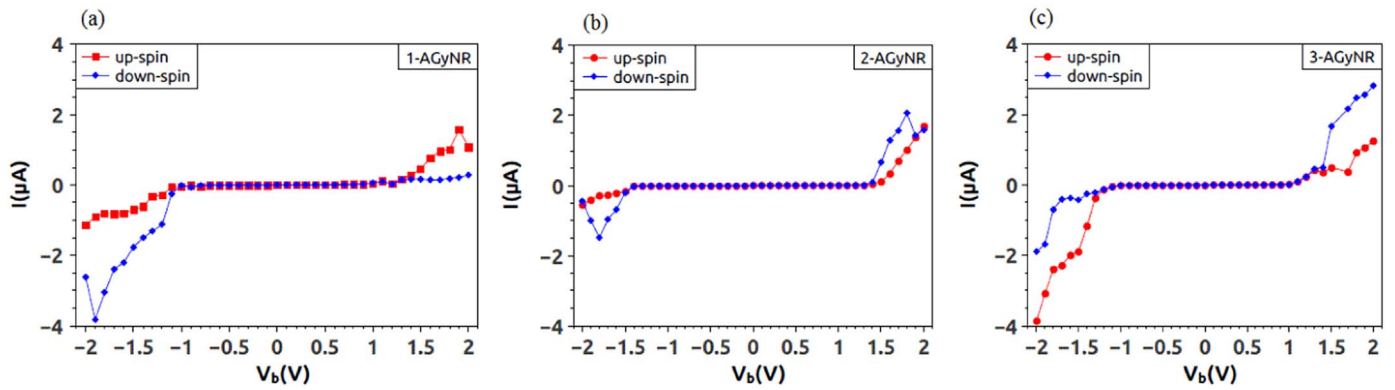


Fig. 6. The spin-polarized  $I$ - $V$  curves of (a)  $n=1$ , (b)  $n=2$  and (c)  $n=3$  Fe-doped AGyNR for both positive and negative bias voltages. The red and blue curves are the current for up spin and down spin electrons, respectively. (For interpretation of the references to color in this figure legend, the reader is referred to the web version of this article.)

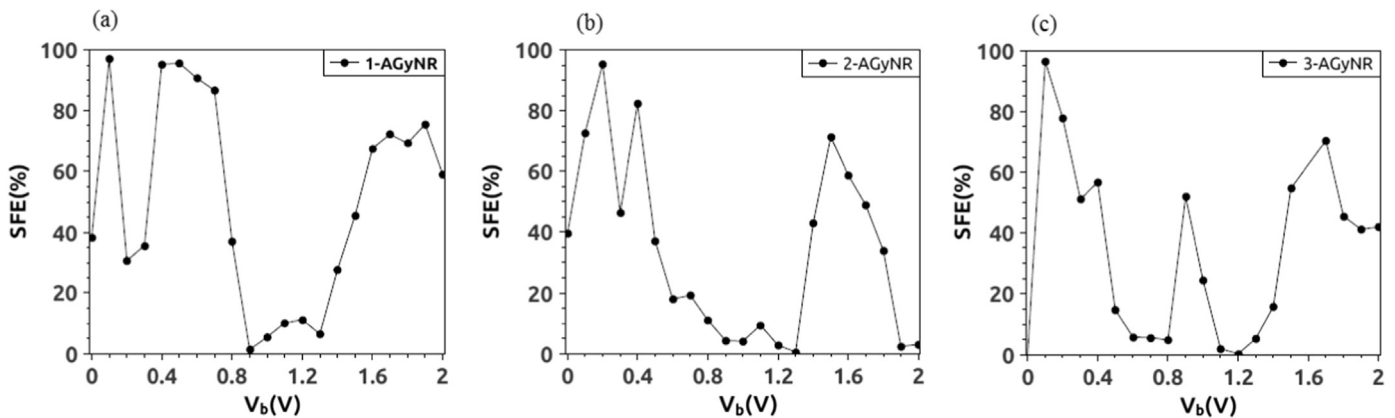


Fig. 7. The bias dependent SFE of (a)  $n=1$ , (b)  $n=2$  and (c)  $n=3$  Fe-doped AGyNR.

( $-2.0, 1.4$  V). However, the case of the down spin electrons is just opposite to that of the up spin electrons and it can easily flow through the device when the negative bias exceeds  $-1.4$  V, while it is blocked within the bias range ( $-1.4, 2.0$  V). This indicates that the Fe-doped 1-AGyNR has both spin filtering and spin-rectifying effects, so it can be applied as a dual spin-filter or a dual spin-diode.

For Fe-doped 2-AGyNR the currents of spin-down electrons increase when the applied bias voltage become higher than  $1.3$  V, and its values are larger than that of the up spin electrons (in inverse proportion to Fe-doped 1-AGyNR). For the up spin electrons, their  $I$ - $V$  curves have flat characteristics and the currents increase slowly with the bias voltage, and it has relatively good spin filtering effect. Moreover, it exhibits no spin-rectifying effect and for negative bias voltages down spin current is dominant.

Similar to previous nanoribbons, Fe-doped 3-AGyNR, the current is considerably spin-polarized and the current of down spin electrons is considerably larger than that of up spin at all bias voltages, particularly after threshold voltage of  $1.1$  V. on the other hand, at almost all bias voltages, the current of up spin electrons, in comparison with the current of down spin electrons, is negligible; indicating its good spin filtering effect. Furthermore, similar to Fe-doped 1-AGyNR by studying the behavior of current in negative voltages, we find its spin-rectifying effect within the applied bias range.

It is mention that, in the case of Fe-doped 1-AGyNR and 2-AGyNR, a negative slope is observable in the  $I$ - $V$  curve between  $1.9$ - $2.0$  V and  $1.8$ - $2.0$  V, respectively which is commonly known as the negative differential resistance (NDR).

To quantify the spin-polarization, we calculated SFE of current, which can be defined by Eq. (1).

It is observed that the SFEs of the systems are extremely depended on the bias voltages and show non-linear behaviors (Fig. 7). The maximum SFEs are  $97.04\%$ ,  $95.42\%$  and  $96.46\%$  for  $n=1$ ,  $n=2$  and  $n=3$  Fe-doped AGyNR at  $0.1$  V,  $0.2$  V and  $0.1$  V, respectively. The large magnitude of spin-filter efficiency in the structures suggested possible applications as spin filters.

Finally, from these results, we can find out that the Fe-doped AGyNRs could have potential application in spintronic.

#### 4. Conclusions

In this paper, the spin-dependent transport properties of Fe-doped armchair graphyne nanoribbons are studied and compared with pure ones. The results show that all pure armchair graphyne nanoribbons have semi-conductive characteristics along the arm-chair direction and in Fe-doped nanoribbons, increasing the amount of electrons caused an impurity state above Fermi level near conductance band of primitive structure. Furthermore, we found that up spin and down spin electronic states are not degenerate. The existence of additional electronic states, from delocalized Fe electrons, across the Fermi level leads to metallicity. Also we found that by increasing the width of nanoribbons, the DOS peaks intensity increases indicating better conductivity. It is obvious that, doping magnetic impurity on studied  $n$ -AGyNRs, has improved the conductance of nanoribbons.

The spin-polarized currents as a function of the applied bias ( $I$ - $V$  curve) for Fe-doped AGyNRs were studied. When the bias voltage becomes larger than the threshold voltage, clearly visible that the current has two parts for up and down spin electrons. This is because the impurity states of doping atom induce extra transport

channels. The current for both up and down spin electrons is considerably spin-polarized; therefore spin-filtering effect can be expected. Threshold voltage decreased by increasing the width of ribbon. For configurations with geometric symmetry spin-rectifying effect was also observed. So they can act as a dual spin-filter or a dual spin-diode in spintronic equipment.

These novel spin-dependent properties of Fe-doped armchair graphyne nanoribbons make them a promising candidate for numerous applications in spintronic devices.

## References

- [1] I. Zutic, J. Fabian, S. Das Sarma, *Rev. Mod. Phys.* 76 (2004) 323.
- [2] A. Fert, *Rev. Mod. Phys.* 80 (2004) 1517.
- [3] XiangHua Zhang, LingLing Wang, XiaoFei Li, Tong Chen, Quan Li, *Phys. Lett. A* 379 (2015) 1722.
- [4] Fu-Bin Yang, Rui Huang, Yan Cheng, *Physica B* 464 (2015) 77.
- [5] Guoliang Sun, J.F. Ding, *J. Magn. Mater.* 394 (2015) 22.
- [6] Minggang Zeng, Lei Shen, Ming Yang, Chun Zhang, Yuanping Feng, *Appl. Phys. Lett.* 98 (2011) 053101.
- [7] Jing Huang, Weiyi Wang, Shangfeng Yang, Haibin Su, Qunxiang Li, Jinlong Yang, *Chem. Phys. Lett.* 539 (2012) 102.
- [8] Chengyong Xu, Linze Li, Hong Li, Rui Qin, Jiixin Zheng, Guangfu Luo, Qihang Liu, Xin Yan, Lili Yu, Jing Lu, Zhengxiang Gao, *Comp. Mater. Sci.* 50 (2011) 2886.
- [9] M. Modarresi, B.S. Kandemir, M.R. Roknabadi, N. Shahtahmasebi, *Phys. B* 445 (2014) 88.
- [10] M. Modarresi, B.S. Kandemir, M.R. Roknabadi, N. Shahtahmasebi, *J. Magn. Mater.* 367 (2014) 81.
- [11] L.D. Pan, L.Z. Zhang, B.Q. Song, S.X. Du, H.J. G., *Appl. Phys. Lett.* 98 (2011) 173102.
- [12] S. Iijima, *Nature* 354 (1991) 56.
- [13] K. Tsukagoshi, B.W. Alphenaar, H. Ago, *Nature* 401 (1999) 572.
- [14] H.W. Kroto, J.R. Heath, S.C. O'Brien, R.F. Curl, R.E. Smalley, *Nature* 318 (1985) 162.
- [15] E.W. Hill, A.K. Geim, K. Novoselov, F. Schedin, P. Blake, *IEEE Trans. Magn.* 42 (2006) 2694.
- [16] C. Jozsa, M. Popinciuc, N. Tombros, H.T. Jonkman, B.J. van Wees, *Phys. Rev. Lett.* 100 (2008) 236603.
- [17] T. Yokoyama, *Phys. Rev. B* 77 (2008) 073413.
- [18] V. Nam, Do, V. Hung Nguyen, P. Dollfus, A. Bournel, *J. Appl. Phys.* 104 (2008) 063708.
- [19] J. Zou, G. Jin, Y.Q. Ma, *J. Phys. Condens. Matter.* 21 (2009) 126001.
- [20] A. Saffarzadeh, M. Ghorbani Asl, *Eur. Phys. J. B* 67 (2009) 239.
- [21] F. Munoz-Rojas, J. Fernandez-Rossier, J.J. Palacios, *Phys. Rev. Lett.* 102 (2009) 136810.
- [22] H. Sahin, R.T. Senger, *Phys. Rev. B.* 78 (2008) 205423.
- [23] M. Modarresi, M.R. Roknabadi, N. Shahtahmasbi, *Phys. E* 43 (2011) 1751.
- [24] N.M.R. Peres, F. Guinea, A.H. Castro Neto, *Phys. Rev. B.* 72 (2005) 174406.
- [25] T.O. Wehling, K.S. Novoselov, S.V. Morozov, E.E. Vdovin, M.I. Katsnelson, A. K. Geim, A.I. Lichtenstein, *Nano Lett.* 173 (2008) 8.
- [26] O.V. Yazyev, L. Helm, *Phys. Rev. B.* 75 (2007) 125408.
- [27] Neeraj K. Jaiswal, Pankaj Srivastava, *Phys. E* 54 (2013) 103.
- [28] Anurag Srivastava, R. Chandiramouli, *Superlattices Microstruct.* 79 (2015) 135.
- [29] M. Kh. Maher, N. Shahtahmasebi, M.R. Roknabadi, *Physica E* 54 (2013) 93.
- [30] M.Y. Han, B. Ozyilmaz, Y.B. Zhang, *Phys. Rev. Lett.* 98 (2007) 206805.
- [31] W.L. Ma, S.S. Li, *Appl. Phys. Lett.* 100 (2012) 163109.
- [32] A.L. Ivanovskii, *Prog. Solid State Chem.* 41 (2013) 1.
- [33] Y. Zhou, J. Zeng, K.Q. Chen, *Carbon* 76 (2014) 175.
- [34] H.W. Kroto, J.R. Heath, S.C. O'Brien, R.F. Curl, R.E. Smalley, *Nature* 3 (1985) 318.
- [35] S. Tanuma, A.V. Palmichenko, N. Satoh, *Synth. Met.* 4 (1995) 1841.
- [36] D. Wei, L. Xie, K.K. Lee, Z. Hu, S. Tan, W. Chen, *Nat. Commun.* 4 (2013) 1374.
- [37] Yan Hong Zhou, Jing Zeng, Ke Qiu Chen, *Carbon* 76 (2014) 175.
- [38] Junjie He, Shuang Ying Ma, Pan Zhou, C.X. Zhang, Chaoyu He, L.Z. Sun, *J. Phys. Chem. C* 116 (2012) 26313.
- [39] M. Kavand, M. Kariminezhad, A. Namiranian, *Solid State Commun.* 150 (2010) 1537.
- [40] Y.Y. Zhang, Q.X. Pei, C.M. Wang, *Comp. Mater. Sci.* 65 (2012) 406.
- [41] Guodong Yu, Zhe Liu, Wenzhu Gao, Yisong Zheng, *J. Phys.: Condens. Matter.* 25 (2013) 285502.
- [42] Jie Tan, Xiujie He, Mingwen Zhao, *Diam. Relat. Mater.* 29 (2012) 42.
- [43] S. Ajori, R. Ansari, M. Mirnezhad, *Mater. Sci. Eng. A—Struct.* 561 (2013) 34.
- [44] T. Ozaki, H. Kino, J. Yu, M. J. Han, N. Kobayashi, M. Ohfuti, F. Ishii, et al., *User's Manual of OpenMX Version3.6*. (<http://www.openmx-square.org>), 2011.
- [45] J.P. Perdew, K. Burke, M. Ernzerhof, *Phys. Rev. Lett.* 77 (1997) 3865.
- [46] H.J. Monkhorst, J.D. Pack, *Phys. Rev. B* 13 (1976) 5188.
- [47] S. Datta, *Electronic Transport in Mesoscopic Systems*, Cambridge University Press, Cambridge, 1995.
- [48] A.V. Rozhkov, G. Giavaras, Yury P. Bliokh, Valentin Freilikher, Franco Nori, *Phys. Rep.* 503 (2011) 77.
- [49] J. Liu, Z.H. Zhang, X.Q. Deng, Z.Q. Fan, G.P. Tang, *Org. Electron.* 18 (2015) 135.
- [50] Juan M. Marmolejo-Tejada, Jaime Velasco-Medina, *Microelectron. J.* 48 (2016) 18.
- [51] Yuhang Jing, Guoxun Wuc, Licheng Guo, Yi Sun, Jun Shen, *Comp. Mater. Sci.* 78 (2013) 22.